Proceeding of the 2013
RSI/ISM International Conference on Robotics and Mechatronics
February 13-15, 2013, Tehran, Iran

Dynamics Modelling and Stable Motion Control of a Ballbot Equipped with a Manipulator

Pouya Asgari[1], Payam Zarafshan[2], S. Ali A. Moosavian[3]
Center of Excellence in Robotics and Control, Advanced Robotics & Automated Systems (ARAS) Lab.
Department of Mechanical Engineering K. N. Toosi Univ. of Technology
PO Box 19395-1999, Fax +98 21 8867 4748, Tehran, Iran
Po.asgari@gmail.com, Payam.zarafshan@gmail.com, Moosavian@kntu.ac.ir

Abstract: Human-Robot physical interaction is an important attribute for robots operating in human environments. A Ballbot is an under-actuated system with nonholonomic dynamic constraints. It is a skinny robot with a small base that helps the robot to move in limited space. It is as tall as human height until could interact by people whereas a Ballbot has not been equipped with a manipulator. This manipulator adds new advantages to the Ballbot such as object manipulation and grasping. In this paper and to achieve more performance of a Ballbot, it is equipped with a PUMA type manipulator which gives to the proposed robot the capability of better stabilization. To this end, dynamics equations of the assumed mobile robot is presented and verified. Then, by respecting to this fact that a Ballbot is in the class of under-actuated systems, a control algorithm is proposed to attain the stable motion control of the system. Finally, a simulation routine is performed to move along the desired path/trajectory. Obtained results reveal the merits of the verified model of the new Ballbot and the considered control algorithm which will be discussed.

Index Terms – Ballbot, Manipulator, Dynamics Modeling, Stability, Motion Control

I. Introduction

Human-Robot physical interaction is an important attribute for robots operating in human environments. A significant, but a frequently overlooked problem is that statically-stable wheeled mobile robots can easily become dynamically unstable. If the center of gravity is too high, or the robot accelerates are too rapidly, or is on a sloping surface, the machine can tip over, [1]. As a Ballbot is an under-actuated system with nonholonomic dynamic constraints, it is a dynamically stable single wheeled mobile robot equipped with an omnidirectional movement. It is skinny and as tall as normal human being, making it more suitable for navigation and interaction in human environment, [2]. Whereas, to add new advantages such as object manipulation task, it should be better that a manipulator is appended to the Ballbot.

In the overall design, mechanism based on an inverse mouse-ball drive, control system, and initial results including dynamic balancing, station keeping, and point-to-point motion were described, [3]. To achieve dynamics equations, authors assumed that the motion in the median capital plane and median coronal plane is decoupled and the equations of motion in these two planes are identical. As a result, they designed a controller for the full 3D system by designing independent controllers for these two separate and identical planar equations of the system, [3]. Nagarajan and et al. presented an integrated planning and control procedure, wherein standard graph-search algorithms are used to plan for the sequence of control policies that will help the system achieve a navigation goal, [4]. Also, they proposed an offline trajectory for body (passive joints) until ball (actuated joints) could reach to its desired configuration with regard to the dynamic constraint. Moreover, a feedback controller is proposed that ensures accurate trajectory tracking. Peng and et al proposed a fuzzy controller for the Ballbot. The major advantage of the proposed fuzzy controller is to dealing with the unknown nonlinearities and external disturbances, [5]. In the same way, a sliding mode control is proposed based on back stepping approach to accomplish robust balancing and agile path tracking of the robot with exogenous disturbances, [6]. Also, computer simulations were added to show the effectiveness of method.

In this paper, we append the Ballbot with a PUMA type manipulator which is the first three PUMA links. It gives the Ballbot new advantages. Also, could use the manipulator to keep balancing the Ballbot and better path/trajectory tracking. So, after we obtain the complete dynamics model of Ballbot with a manipulator by Lagrange method, it is verified by Kane method. Next, Static stable motion control of the system is performed for keeping the system stable. At last, the simulation routine is performed to move along the desired path. Obtained results of the implementation of this controller on the Ballbot will be discussed.

II. Dynamics Equations of Motion

In this section, first the system structure and the physical configuration of the assumed Ballbot is describe. Then, the dynamics modelling of the robot is presented using Lagrangian mechanics and Kane's method. Then, verification was done by comparison of these 2 methods' results. Note that the modeling process is based on these simplification assumptions: the Ballbot is constructed by two major components of the ball and

1- MSc Student
2- PhD
3- Professor

978-1-4673-5811-8/13/$31.00 ©2013 IEEE

body. Also, there is no slip between the ball and body and the friction was neglected.

To describe the dynamics of the robot, a reference coordinate XYZ is selected. The robot have 7 DOFs, consist of a ball with 2 DOFs, 2 DOFs for cylinder (roll and pitch of base, [7]) and a manipulator with 3 DOF. The reference coordinate is selected as shown in Fig. 1. Also, θ_1 and θ_2 are considered as ball rotations about Y and X directions, respectively. For body rotations, θ_3 and θ_4 are considered as roll and pitch angles of base as shown in Fig. 1.

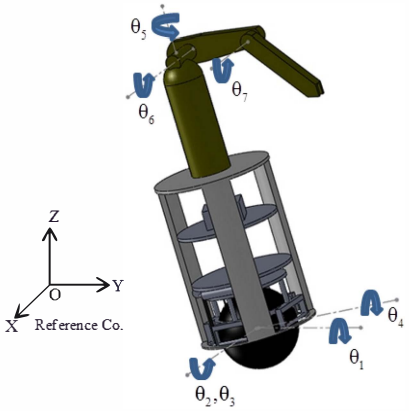

Fig 1 – Definition of the reference and generalized coordinates

The manipulator with 3 DOFs is the first three PUMA joints. The Denavit-Hartenberg notation is used to select frames for manipulator rotations, [8]. As shown in Fig. 2, rotations are done about z_5, z_6 and z_7 equal to θ_5, θ_6 and θ_7, respectively.

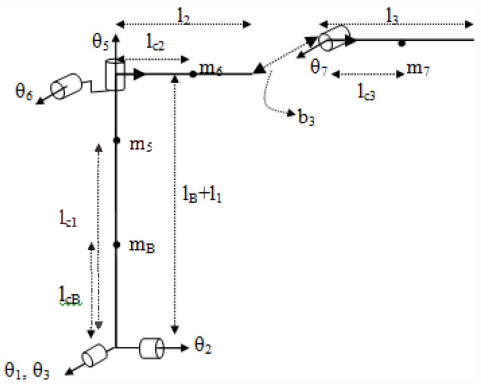

Fig 2 – Schematic of the assumed Ballbot and its coordinates

The transformation matrix of body rotation is:

$$ {}^{0}_{4}T=\begin{bmatrix} c_4 & 0 & s_4 & r_b\theta_1 \\ s_4s_3 & c_3 & -s_3c_4 & -r_b\theta_2 \\ -s_4c_3 & s_3 & c_4c_3 & 0 \\ 0 & 0 & 0 & 1 \end{bmatrix} \qquad (1) $$

where r_b is radius of ball. In addition, the Denavit-Hartenberg schedule for manipulator is shown in Table 1. The angular velocity of coordinate 4 is expressed by:

$$ {}^{0}\boldsymbol{\omega}^{0}_{4}=\begin{pmatrix} \dot{\theta}_3 & \dot{\theta}_4\cos\theta_3 & \dot{\theta}_4\sin\theta_3 \end{pmatrix}^{\mathrm{T}} \qquad (2) $$

Also, the angular velocities of coordinate 5, 6 and 7 relative to earlier coordinate and expressed in reference coordinate are:

$$ \boldsymbol{\omega}_i = {}^{0}_{i}R\begin{bmatrix} 0 & 0 & \dot{\theta}_i \end{bmatrix}^{T} \qquad i=5,6,7 $$
$$ {}^{0}_{i}T = {}^{0}_{4}T....{}^{i-1}_{i}T \qquad (3) $$

Where ${}^{i-1}_{i}T$ is obtained from transformation matrix [8]

TABLE I. - DENAVIT-HARTENBERG PARAMETERS OF MANIPULATOR

i	A	α	D	θ
5	0	0	l_B+l_1	θ_5
6	0	$\pi/2$	0	θ_6
7	l_2	0	$-b_3$	θ_7

The velocity of mass j refers to reference coordinate is computed as:

$$ \mathbf{v}_j = \mathbf{v}_b + \sum_{i=4}^{j}\boldsymbol{\omega}_i \times {}^{0}\mathbf{R}^{i}_{j} \quad \text{for} \quad j=4,5,6,7 \qquad (4) $$

where $\mathbf{v}_b$ is the velocity of ball. The ball is actuated by a pair of smooth stainless steel rollers placed orthogonally at the sphere's equator [3]. The arm's link is rotated by motors that apply torque to each links. Speed on the surface of the ball (in rollers direction) has to be the same speed as the tangential speed of the omniwheels. Thus:

$$ \dot{\varphi}_{1y} = -\frac{r_b}{r_s}C_3\dot{\theta}_1+\frac{(r_b+r_s)}{r_s}\dot{\theta}_4 $$
$$ \dot{\varphi}_{2x} = -\frac{r_b}{r_s}S_4S_3\dot{\theta}_1-\frac{r_b}{r_s}C_4\dot{\theta}_2+\frac{(r_b+r_s)}{r_s}C_4\dot{\theta}_3 \qquad (5) $$

where r_s is radius of rollers, $\dot{\varphi}_{1y}$ and $\dot{\varphi}_{2x}$ are the velocity of drive rollers. Non potential forces for the first four lines of Lagrange equations are calculated as, [9]:

$$ \frac{\partial(-\tau_1\dot{\varphi}_{2x}-\tau_2\dot{\varphi}_{1y})}{\partial\dot{\theta}_i}+\mathbf{J}_{CT}{}^{\mathrm{T}}\begin{bmatrix}\tau_1 & \tau_2 & 0\end{bmatrix}^{\mathrm{T}} \qquad i=1,...,4 \qquad (6) $$

where:

$$ \mathbf{J}_{CT}=\begin{bmatrix} 0 & 0 & c_4 & 0 \\ 0 & 0 & 0 & 1 \\ 0 & 0 & s_4 & 0 \end{bmatrix} \qquad (7) $$

So, non-potential forces for system are (with arm):

$$ \boldsymbol{\tau}=\begin{bmatrix} \frac{r_b}{r_s}s_3s_4\tau_1+\frac{r_b}{r_s}c_3\tau_2 & \frac{r_b}{r_s}c_4\tau_1 & -\frac{r_b}{r_s}c_4\tau_1 & -\frac{r_b}{r_s}\tau_2 & \tau_5 & \tau_6 & \tau_7 \end{bmatrix}^{\mathrm{T}} \qquad (8) $$

where τ_1 τ_2 are torques of rollers and τ_5, τ_6, τ_7 are torques of manipulator. It should be noted that system parameters are explained in Table 2.

TABLE II. – THE ASSUMED BALLBOT SPECIFICATIONS AND PARAMETERS

Length (m)	r_b	Ball radius	0.2
	r_s	Roller radius	0.01
	l_B	Body length	1
	l_1	First manipulator's link	0.5
	l_2	Second manipulator's link	0.5
	l_3	Third manipulator's link	0.5
	b_3	Distance between Co. 6 and 7	0.1
Weight (kg)	m_b	Mass of ball	0.5
	m_B	Mass of body	2
	m_5	Mass of First manipulator's link	0.5
	m_6	Mass of Second manipulator's link	0.5
	m_7	Mass of Third manipulator's link	0.5
Inertia (kg.m2)	I_b	Inertia of ball	0.008
	I_{xxB}, I_{yyB} I_{zzB}	Inertia of body	0.167 0
	I_{xx1}, I_{yy1} I_{xx3}	Inertia of First manipulator's link	0.0104 0
	I_{yy2}, I_{zz2} I_{xx2}	Inertia of Second manipulator's link	0.0104 0
	I_{yy3}, I_{zz3} I_{xx3}	Inertia of Third manipulator's link	0.0104 0

A. Lagrange's Equations

The forced Lagrange equations of motion for a mechanical system are, [10]:

$$\frac{d}{dt}\left(\frac{\partial L}{\partial \dot{q}}\right) - \frac{\partial L}{\partial q} = F(q)\tau \tag{9}$$

Where $q \in \mathbb{R}^n$, $L(q,\dot{q}) = T(q,\dot{q}) - V(q)$, T, V, $\tau \in \mathbb{R}^m$ and $F(q) \in \mathbb{R}^{n\times m}$ are configuration vector, Lagrangian, kinetic energy, potential energy, control inputs and force matrix, respectively. The kinetic energy of the system is computed by:

$$T = 0.5\left(\sum (m_i \mathbf{V}_i^T \mathbf{V}_i + \boldsymbol{\omega}_i^T I_i \boldsymbol{\omega}_i)\right) \tag{10}$$

Where m_i refer to the mass of link *i*, $\mathbf{V}_i$ refer to velocity of the link *i*, $\boldsymbol{\omega}_i$ refer to angular velocity of the link *i* and I_i refer to inertia of link *i* all in reference coordinate. Also, the potential energy of the system is computed as:

$$V = \sum (m_i \mathbf{g}^T \bar{R}_i) \tag{11}$$

where $\mathbf{g} = [0 \quad 0 \quad 9.81]^T$ and ${}^0\bar{\mathbf{R}}_i$ is the center gravity's position of link i refer to coordinate 0. It should be note that the Ball rotates on the ground, so, its potential energy is zero.

B. Kane's Equations

Kane's equations can be derived from D'Alembert's principle. An advantage of Kane's equations is that the approach, especially the use of partial velocities, is desirable of interconnected and large-order systems. Kane's equations are obtained by taking dot product of $m\mathbf{a}_G$ with $\mathbf{v}_G^k$ and $\dot{\mathbf{H}}_G$ with $\boldsymbol{\omega}^k$ and summing the two expressions. These results in the equation of the motion for the k-th generalized speed. In essence, the k-th equation is simply the sum of the components of the forced and moment balance along the direction of the partial velocities. This interpretation should be compared with the interpretation of Lagrange's equations in term of the Euler angles, [11]. For a system of N bodies, this principle is written in term of the generalized velocities as:

$$\sum_{i=1}^{N} (\mathbf{v}_{Gi}^k . m_i \mathbf{a}_{Gi} + \boldsymbol{\omega}_i^k . \dot{\mathbf{H}}_{Gi}) = \mathbf{Q}_k \quad for\ k = 1, ..., n$$
$$\mathbf{v}_G^k = \frac{\partial \mathbf{v}_G}{\partial u_k} \qquad \boldsymbol{\omega}^k = \frac{\partial \boldsymbol{\omega}}{\partial u_k} \tag{12}$$

where $N, n, \mathbf{V}_{Gi}, \mathbf{a}_{Gi}, \boldsymbol{\omega}_i, \dot{\mathbf{H}}_{Gi}$ and $\mathbf{Q}_k$ are number of mass, number of generalized coordinates, velocity of mass, acceleration of mass, angular velocity of mass, rate of rotational momentums and generalized forces, correspondingly, [11].

For satisfying Eq. 12, velocity and acceleration of each mass should be calculated. Mass velocities can be computed based on generalized velocities as:

$$\mathbf{v}_i = \begin{bmatrix} \mathbf{v}_{Gi} \\ \boldsymbol{\omega}_i \end{bmatrix} = J_i \dot{q}$$
$$\dot{q} = [\dot{\theta}_1 \quad \dot{\theta}_2 \quad \dot{\theta}_3 \quad \dot{\theta}_4 \quad \dot{\theta}_5 \quad \dot{\theta}_6 \quad \dot{\theta}_7]^T \tag{13}$$

where , $\mathbf{v}_{Gi} \in \mathbb{R}^{3\times 1}$ is linear velocity, $\boldsymbol{\omega}_i \in \mathbb{R}^{3\times 1}$ is angular velocity, $J_i \in \mathbb{R}^{6\times 7}$ is Jacobian matrix and $\dot{q} \in \mathbb{R}^{7\times 1}$ is generalized velocity. Furthermore, acceleration of masses can be computed by:

$$\mathbf{a}_i = \begin{bmatrix} \mathbf{a}_{Gi} \\ \boldsymbol{\alpha}_i \end{bmatrix} = \dot{J}_i \dot{q} + J_i \ddot{q} \tag{14}$$

where $\mathbf{a}_{Gi} \in \mathbb{R}^{3\times 1}$ is linear acceleration, $\boldsymbol{\alpha}_i \in \mathbb{R}^{3\times 1}$ is angular acceleration. Also, rate of rotational momentums should be achieved as:

$$\dot{\mathbf{H}}_{Gi} = I_i \boldsymbol{\alpha}_i + \boldsymbol{\omega}_i \times I_i \boldsymbol{\omega}_i \qquad (15)$$

where I_i is inertia matrix of mass i.

C. Model Verification

In this section, two analytical methods (Lagrange and Kane) are used to show the verification of the model. The Dynamics model is verified by comparison of the simulation results of Kane and Lagrange extracted dynamics model. Considering the system parameters of Table 2 in the simulation routine, torques of each joint that are calculated (Fig. 3). Also, model verification errors of Kane and Lagrange comparison is shown in Fig. 4 which have lowest errors and complete the verification procedure. Periodic trajectories have been assumed for each joint to display the torque diagram of active joints as (i.e., trajectories of body rotations (θ_3,θ_4) is confined to $\pm 6^\circ$):

$$\begin{aligned} \theta_1 &= 6\sin(t/2\pi) & \theta_2 &= 6\sin(t/2\pi) \\ \theta_3 &= 0.1\sin(t/2\pi) & \theta_4 &= 0.1\sin(t/2\pi) \\ \theta_5 &= 6\sin(t/2\pi) & \theta_6 &= 6\sin(t/2\pi) \\ \theta_7 &= 6\sin(t/2\pi) \end{aligned} \qquad (16)$$

As shown in these Figures, they are completely the same with no errors. So, dynamics equations of motion which are calculated by Lagrange and Kane methods are comply perfectly.

III. Controller Design

The Ballbot is an underactuated system with dynamic constraints. Trajectory planning and control of underactuated mechanical systems, systems with fewer control inputs than the number of generalized coordinates, has attracted growing attention over the years, [2]. Underactuated systems contain both active and passive joints in a serial kinematics chain. The study of underactuation is significant for the control of a variety of robotic systems, such as free-floating robots in space, whose structure include passive joints, [12-14]. Nonlinearities and time dependencies in the system dynamics of mechanical manipulators make control of these systems the one of the most complicated problem.

Wheeled mobile manipulators and humanoid robots use body articulation to improve performance and balance [15-18]. A simple controller for robot motion and an optimization method for choosing its parameters were presented in [19]. It presented a PD controller for the height of the upper link centre of mass. While in this paper, static stability of system was presented. We control the centre of mass to move the ball in desired path. The manipulator motion was used to keep the centre of mass of system upper the centre of ball. So, with low acceleration of the centre of gravity, system is moved in desired trajectory.

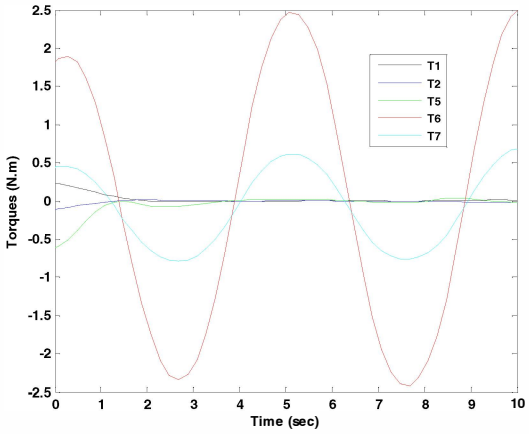

Fig. 3 – Calculated actuator torques of each joint

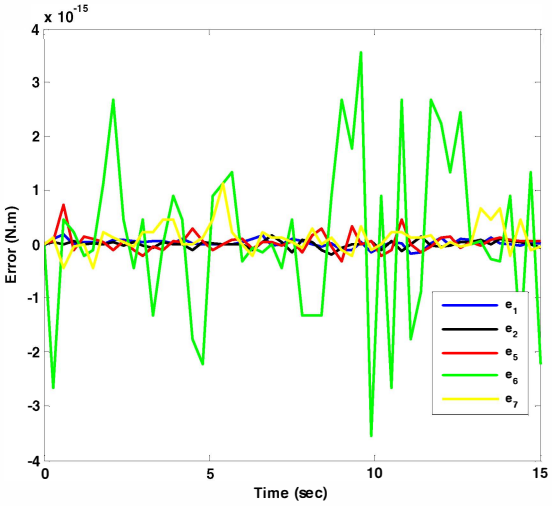

Fig. 4 – Comparison results of Lagrange and Kane method

We would like to put the centre of mass at upper the ball and control the position of ball on the ground. It is obvious that position of ball and centre of gravity are function of joints space. In other word: To find the acceleration of ball and mass center, we compute the second derivative of positions with respect to time. These give linear equations in $\ddot{\mathbf{q}}$ with some additional terms, D, due to velocities. By considering a simple PD controller, we will have:

$$\begin{aligned} \ddot{\bar{x}} &= h_1(\mathbf{q},\dot{\mathbf{q}},\ddot{\mathbf{q}}) = k_{p1}(\bar{x}_{des} - \bar{x}) + k_{v1}(\dot{\bar{x}}_{des} - \dot{\bar{x}}) \\ \ddot{\bar{y}} &= h_2(\mathbf{q},\dot{\mathbf{q}},\ddot{\mathbf{q}}) = k_{p2}(\bar{y}_{des} - \bar{y}) + k_{v2}(\dot{\bar{y}}_{des} - \dot{\bar{y}}) \\ \ddot{x}_{ball} &= r_b\ddot{\theta}_1 = k_{p3}(x^{des}_{ball} - x_{ball}) + k_{v3}(\dot{x}^{des}_{ball} - \dot{x}_{ball}) \\ \ddot{y}_{ball} &= -r_b\ddot{\theta}_2 = k_{p4}(y^{des}_{ball} - y_{ball}) + k_{v4}(\dot{y}^{des}_{ball} - \dot{y}_{ball}) \end{aligned} \qquad (17)$$

where k_{pi} and k_{vi} are controller gains. So, these equations can be written as:

$$\mathbf{w}\ddot{\mathbf{q}} + \mathbf{D} = \mathbf{s} \qquad (18)$$

where $\mathbf{s}$ is PD controller. Then, dynamic equations of motion were calculated in previous section as follows:

$$\mathbf{M\ddot{q} + V + G = B\tau}$$
$$\boldsymbol{\tau} = [\,\tau_1 \quad \tau_2 \quad \tau_3 \quad \tau_4 \quad \tau_5\,]^T \tag{19}$$

These equations could be written as follows:

$$\mathbf{B^{-1}M\ddot{q} + B^{-1}(V + G) = \tau} \tag{20}$$

The control equations are constructed to balance the robot and make the ball to move on desired trajectory. We add Eq. 18 to Eq. 20, as a result:

$$\mathbf{W(q)\ddot{Q} = S} \tag{21}$$

where:

$$\mathbf{W} = \begin{bmatrix} \mathbf{B^{-1}M} & \mathbf{-I_{5\times5}} \\ \mathbf{w} & \mathbf{0_{4\times5}} \end{bmatrix}, \ddot{\mathbf{Q}} = \begin{bmatrix} \ddot{\mathbf{q}} \\ \boldsymbol{\tau} \end{bmatrix}, \mathbf{S} = \begin{bmatrix} \mathbf{B^{-1}(V+G)} \\ \mathbf{s - D} \end{bmatrix} \tag{22}$$

By Inverting the augmented matrix $\mathbf{W}$, the desired solution for accelerations and torques is resulted. We directly apply this torques to our system.

IV. Simulation Results And Discussion

The goal of the control algorithm is to move the ball on desired path and keep the center of gravity at upper the ball. The ball should be moved from $(x,y)_0 = (0,0)$ to $(x,y)_f = (5,4)$. So, a linear function with parabolic blends trajectory was planned [18]. Also desired position of center of gravity relative to ball position is zero. So, desired X and Y trajectories of ball will be as:

$$x(t) = \begin{cases} 0.156t^2 & 0 \le t \le 2 \\ 0.625(t-2) + 0.25 & 2 \le t \le 8 \\ -0.156(10-t)^2 + 5 & 8 \le t \le 10 \end{cases}$$
$$y(t) = \begin{cases} 0.125t^2 & 0 \le t \le 2 \\ 0.5(t-2) + 0.5 & 2 \le t \le 8 \\ -0.125(10-t)^2 + 4 & 8 \le t \le 10 \end{cases} \tag{23}$$

Therefore, the center of gravity position and its acceleration, the position of ball and the ball rotations are shown in Figures (5-8).

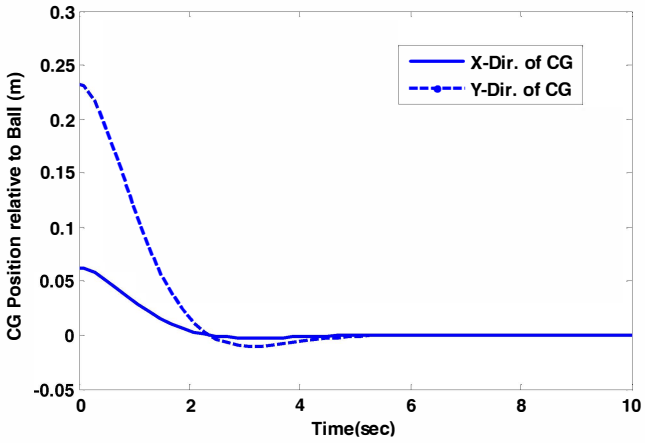

Fig 5 – Center of gravity position to perform stable motion control

So, actuator torques which is applied to active joints results in the Center of Gravity (CG) position which is controlled (Fig. 5). This means that the CG position is coincided on the ball position and consequently, the stable motion control is attained. In addition, this stable motion control is successful when the CG acceleration is converged to zero too. This fact is perfectly achieved by the designed stable motion controller which is shown in Fig. 6. Moreover, the ball is tracked the designed path in this procedure (Fig. 7). Rotation of ball in joint space is shown Fig. 8. In addition, an animated view of the system performing the stable motion control task along the desired path is shown in Fig. 9.

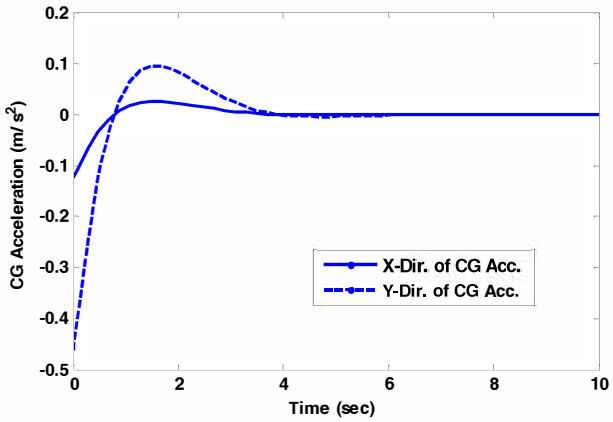

Fig. 6 – Center of gravity acceleration to perform stable motion control

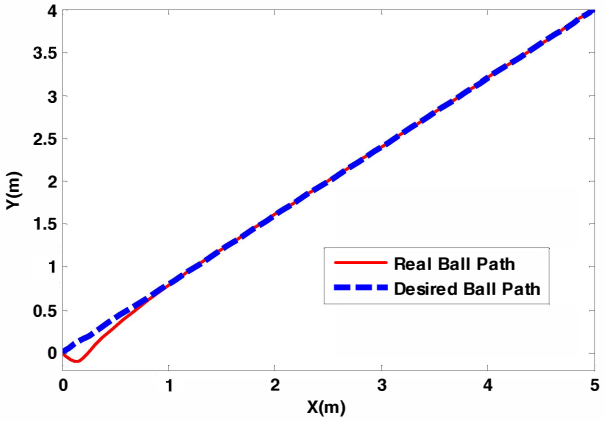

Fig. 7 – Ball position to perform stable motion control

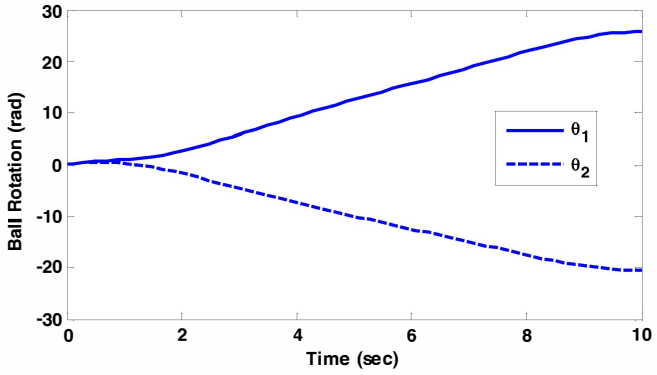

Fig. 8 – Illustration of ball rotation to keep Ballbot stability

V. CONCLUSIONS

This paper was presented dynamics model and stable motion control of a Ballbot which is equipped with a manipulator. Manipulator could help the Ballbot to control its stability. Validation of dynamics equations was performed by comparison of two analytical methods. Coincidence of these two methods showed validation of the model. To apply a stable motion control, a controller was used to control the whole system. This action was done by controlling the ball position and position of centre of gravity of system. Finally, simulation results were shown that the proposed control scheme could control the system well

REFERENCES

[1] T. Lauwers, G. A. Kantor, and R. Hollis, "A dynamically stable single-wheeled mobile robot with inverse mouse-ball drive," in Proceedings of the IEEE International Conference on Robotics and Automation, Orlando, FL, USA, 2006, pp. 2884-2889.

[2] U. Nagarajan, G. Kantor, and R. L. Hollis, "Trajectory planning and control of an underactuated dynamically stable single spherical wheeled mobile robot," in Proceedings of the IEEE International Conference on Robotics and Automation, Kobe, Japan, 2009, pp. 3743-3748

[3] T. Lauwers, G. Kantor, and R. Hollis, "One is enough!," Robotics Research, pp. 327-336, 2007

[4] U. Nagarajan, G. Kantor, and R. Hollis, "Hybrid control for navigation of shape-accelerated underactuated balancing systems," in 49th IEEE Conference on Decision and Control, Atlanta, GA, 2010, pp. 3566-3571.

[5] Y. F. Peng, C. H. Chiu, W. R. Tsai, and M. H. Chou, "Design of an Omni-directional Spherical Robot: Using Fuzzy Control," 2009

[6] C. W. Liao, C. C. Tsai, Y. Y. Li, and C. K. Chan, "Dynamic modelling and sliding-mode control of a Ball robot with inverse mouse-ball drive," in SICE Annual Conference, Tokyo, Japan, 2008, pp. 2951-2955.

[7] L. Meirovitch, Methods of analytical dynamics: Dover Publications, 2010

[8] J. J. Craig, "Introduction to Robotics. Mechanics and Control. Series in Electrical and Computer Engineering: Control Engineering," ed: Addison-Wesley, Reading, MA, USA, 1989.

[9] P. Fankhauser and C. Gwerder, "Modeling and Control of a Ballbot," Bachelor's thesis, University of ETH, Zurich, Swiss, 2010.

[10] U. Nagarajan, "Dynamic constraint-based optimal shape trajectory planner for shape-accelerated underactuated balancing systems," 2010.

[11] H. Baruh, Analytical dynamics: WCB/McGraw-Hill, 1999.

[12] R. Mukherjee and D. Chen, "Control of free-flying underactuated space manipulators to equilibrium manifolds," Robotics and Automation, IEEE Transactions on, vol. 9, pp. 561-570, 1993.

[13] S. A. A. Moosavian and E. Papadopoulos, "Free-flying robots in space: an overview of dynamics modeling, planning and control," Robotica, vol. 25, pp. 537-547, 2007.

[14] M. D. Berkemeier and R. S. Fearing, "Tracking fast inverted trajectories of the underactuated acrobot," Robotics and Automation, IEEE Transactions on, vol. 15, pp. 740-750, 1999.

[15] K. Alipour and S. A. A. Moosavian, "Point-to-point stable motion planning of wheeled mobile robots with multiple arms for heavy object manipulation," in IEEE International Conference on Robotics and Automation (ICRA), Shanghai, 2011, pp. 6162-6167.

[16] S. Kajita, F. Kanehiro, K. Kaneko, K. Fujiwara, K. Harada, K. Yokoi, and H. Hirukawa, "Biped walking pattern generation by using preview control of zero-moment point," in Proceedings of the IEEE International Conference on Robotics and Automation, 2003, pp. 1620-1626.

[17] K. Nishiwaki, S. Kagami, Y. Kuniyoshi, M. Inaba, and H. Inoue, "Online generation of humanoid walking motion based on a fast generation method of motion pattern that follows desired zmp," in Proceedings IEEE/RSJ International Conference on Intelligent Robots and Systems, 2002, pp. 2684-2689.

[18] K. Harada, S. Kajita, F. Kanehiro, K. Fujiwara, K. Kaneko, K. Yokoi, and H. Hirukawa, "Real-time planning of humanoid robot's gait for force-controlled manipulation," Mechatronics, IEEE/ASME Transactions on, vol. 12, pp. 53-62, 2007.

[19] M. Stilman, J. Wang, K. Teeyapan, and R. Marceau, "Optimized control strategies for wheeled humanoids and mobile manipulators," in Proceedings of the IEEE-RAS International Conference on Humanoid Robots, Paris, 2009, pp. 568-573.

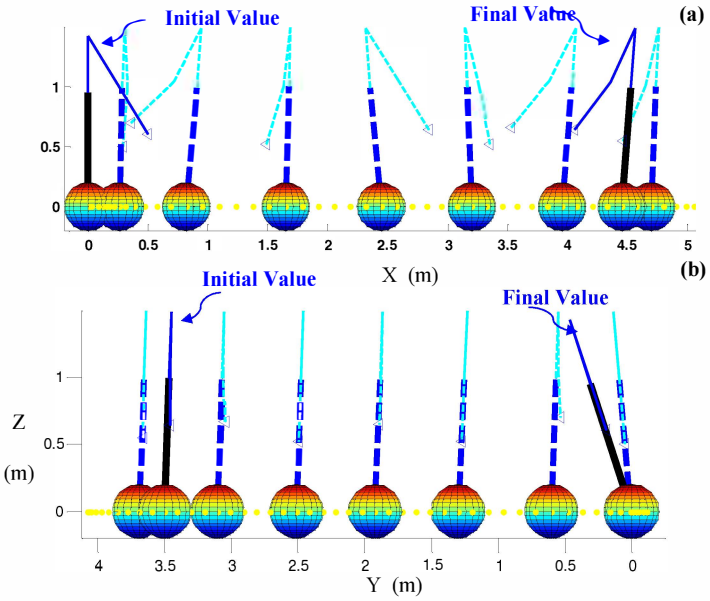

Fig. 9 – Animated view of the system performing the stable motion control task: (a) X-Z view - (b) Y-Z view